Homochirality to design high-T_c lead-free ferroelastic semiconductor

Bo-Wen Deng[a], Zhi-Peng Rao[a], Ming-Jing Shen[a], Ke-Wei Liang[c], Yang Zhu[a], Zhi-Jie Wang[a], Kun Ding[a], Chang-Yuan Su[a], Meng-Meng Lun[a], Zhi-Xu Zhang[b*], Yi Zhang[b*], Da-Wei Fu[a*]

[a] Ordered Matter Science Research Center, Jiangsu Key Laboratory for Science and Applications of Molecular Ferroelectrics, Southeast University, Nanjing, 211189, People's Republic of China. Email: dawei@zjnu.edu.cn

[b] Institute for Science and Applications of Molecular Ferroelectrics, Key Laboratory of the Ministry of Education for Advanced Catalysis Materials, Zhejiang Normal University, Jinhua, 321019, People's Republic of China. Email: zhangzhixu@zjnu.edu.cn, yizhang1980@seu.edu.cn

[c] School of Electronic and Communication Engineering, Tianjin Normal University, Tianjin 300387, People's Republic of China.

Experimental Measurement Methods

Single-crystal X-ray crystallography (SXRD):

The single-crystal structure is the most direct way to determine crystal structure. X-diffraction of compounds (*R*/*S*-CTA)$_2$SbCl$_5$ and TMCP$_2$SbCl$_5$ at 293 K was performed to obtain crystallographic data of the compound mass (using Rigaku VarimaxTM DW diffractometer and MoKα radiation (λ=0.71073Å)). The crystallographic data were processed by direct methods and refined by full matrix least squares using the SHLXTL-2014 program. The non-H atoms were refined an isotropically, limiting all reflections to I>2σ(I); moreover, the rational positions of the H atoms were geometrically generated and refined with the " riding" model (Uiso(H) = 1.2 Ueq (C or N))

Differential scanning calorimetry (DSC):

The (*R*/*S*-CTA)$_2$SbCl$_5$ and TMCP$_2$SbCl$_5$ powders were sealed in an aluminum crucible to preform DSC and tested from 330 K to 440 K under nitrogen protection using netzsch-214 DSC.

Dielectric:

Tonghui TH2828A Precision LCR Meter was used to measure the dielectric response of (*R*/*S*-CTA)$_2$SbCl$_5$ and TMCP$_2$SbCl$_5$. The samples were pressed into sheets, coated with silver glue on both sides, and tested at 500 kHz-1 MHz frequency and 1V AC voltage.

Ultraviolet–visible (UV–vis) absorption:

Ultraviolet–visible (UV-vis) absorption spectroscopy measurements on (*R*/*S*-CTA)$_2$SbCl$_5$ and TMCP$_2$SbCl$_5$ (polycrystalline samples) were performed at room temperature using a Shimadzu (Tokyo, Japan) UV-2600 spectrophotometer with an ISR-2600Plus integrating sphere in the range of 200–400 nm. $BaSO_4$ was used as the 100% reflectance reference.

Second-harmonic generation (SHG):

The compounds were prepared into powders with different particle sizes for SHG response testing. Temperature-varying SHG experiments were performed by using a low-divergence basic laser beam, which pulsed in Nd: YAG. The wavelength is 1064 nm, the peak power is 1.6 MW, the repetition rate is 10 Hz, and the pulse duration is 5 ns.

Powder X-ray Diffraction (PXRD):

X-ray diffraction patterns of the microcrystalline compounds were characterized at room temperature using a Rigaku D/MAX diffraction system under Cu-Kα radiation with a diffraction range of 5-50° and a step size of 0.02°. At the same time, the X-ray diffraction patterns of the samples were tested in the temperature range of 293-435 K. In conjunction with the crystallographic information files from the variable temperature X-ray powder diffraction experiments, the space groups of the crystals were simulated using the material studio software package.

Hirshfeld Surfaces analysis:

Hirshfeld d_{norm} surfaces and 2D fingerprint plots surrounding inorganic anions were calculated by the CrystalExplorer software based on their SC-XRD data. Hirshfeld surfaces with d_{norm} values reveal a red-blue-white color scheme that imply the intensity of intermolecular interactions, of which the red/blue/white regions mean that intermolecular interactions are stronger/equal/weaker compared to the van der Waals forces. In 2D fingerprint plots, each point represents an individual pair (*d*i, *d*e), reflecting the distances to the nearest atom inside (*d*i) and outside (*d*e) of the Hirshfeld d_{norm} surface.

Density Functional Theory (DFT) Calculations:

The band structure and partial density state were performed based on density function theory (DFT) by using the Vienna Ab-initio Simulation Package (VASP). Firstly, the crystallographic structures of compounds obtained from SC-XRD measurement were further optimized geometrically, employing the exchange-correlation interactions within the generalized gradient approximation (GGA) on the basis of the Perdew Burke Ernzerh (PBE) function. Secondly, the band structure and partial density state of optimized structures were calculated by the PBE function with considering spin-orbit coupling (SOC) and without considering SOC, respectively. Meanwhile, the plane wave cut-off energy, the force and energy convergence criterions were set to be 520 eV, 0.02 eV/Å and 10^{-6} eV per atom, respectively, and the mesh samplings in the Brillouin zone were 1 × 1 × 2 for (*R*/*S*-CTA)$_2$SbCl$_5$ and TMCP$_2$SbCl$_5$. In addition, the other parameters and convergent criteria were the default values. Finally, the post-processing analysis was performed by using VASPKIT.

Ferroelastic Measurement:

The evolution of ferroelastic domains for (*R*-CTA)$_2$SbCl$_5$ crystals was observed by an Olympus BX51TRF polarizing microscope equipped with temperature control INSTEC HCC602

Synthesis:

The reagents and solvents designed in this experiment are analytical pure and do not require further purification.

(TMCP)Cl

Prepare a 250 mL round bottom flask, add 0.12 mol 1,3-Dichloropropane, 0.1 mol trimethylamine alcohol solution, and 100 mL acetonitrile to the flask for mixing. Heat the mixed solution in an oil bath at 323 K for 12 hours. After the reaction is complete, perform vacuum distillation on the mixed solution to obtain a white powder. Dry the white powder in an oven at 323 K for 2 hours to obtain (TMCP)Cl.

$TMCP_2SbCl_5$ and (R/S-CTA)$_2SbCl_5$

$TMCP_2SbCl_5$ and (R/S-CTA)$_2SbCl_5$ were synthesized using the solvent evaporation method. Mix (TMCP)Cl, R/S-CTA, and $SbCl_3$ with a molar ratio of 4:2, dissolve them in a 37% hydrochloric acid aqueous solution, and evaporate them on a 318 K hot plate for 5 days to obtain white transparent crystals of TMCP and(R/S-CTA)$_2SbCl_5$. The room temperature powder X-ray diffraction (PXRD) patterns of $TMCP_2SbCl_5$ and (R/S-CTA)$_2SbCl_5$ match well with the simulated data based on the 273 K crystal structure (Fig. S1). This can prove the phase purity of $TMCP_2SbCl_5$ and (R/S-CTA)$_2SbCl_5$.

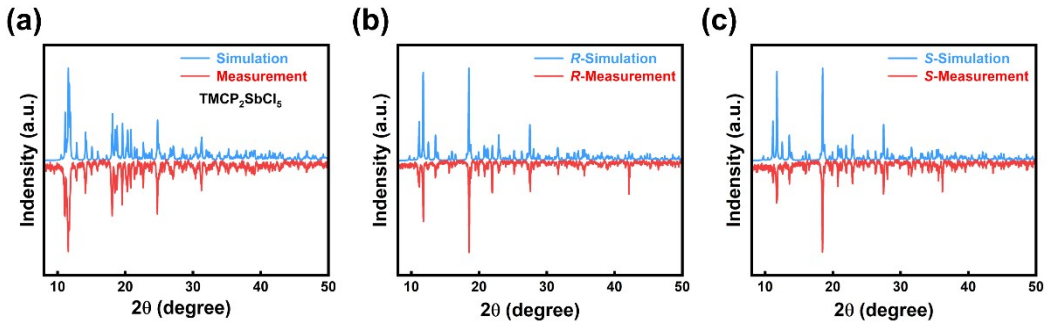

Fig. S1 The powder XRD of $(TMCP)_2SbCl_5$ (a), (R-CTA)$_2SbCl_5$ (b), and (S-CTA)$_2SbCl_5$ (c) with the simulated one in blue and the measurement in red.

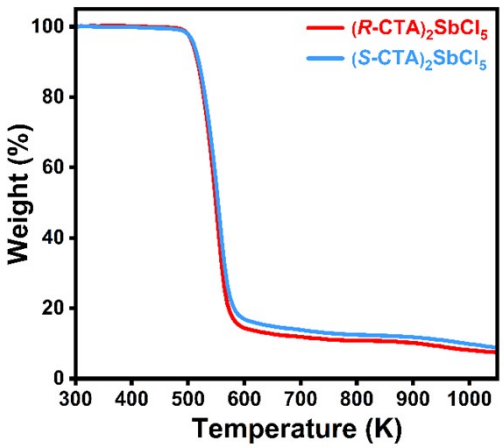

Fig. S2 TGA curve of (R/S-CTA)$_2SbCl_5$

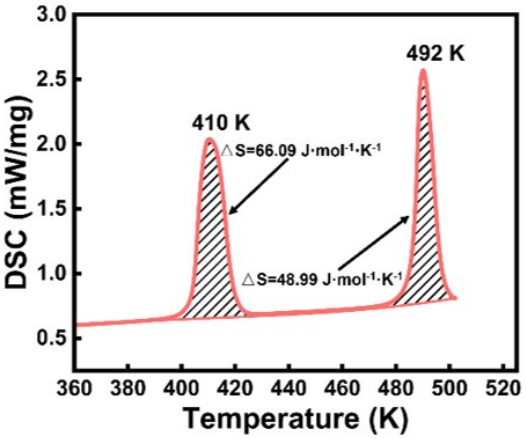

Fig. S3 The heating DSC curve of (S-CTA)$_2$SbCl$_5$ (b). The enthalpy change of plastic phase transition is greater than the melting enthalpy change.

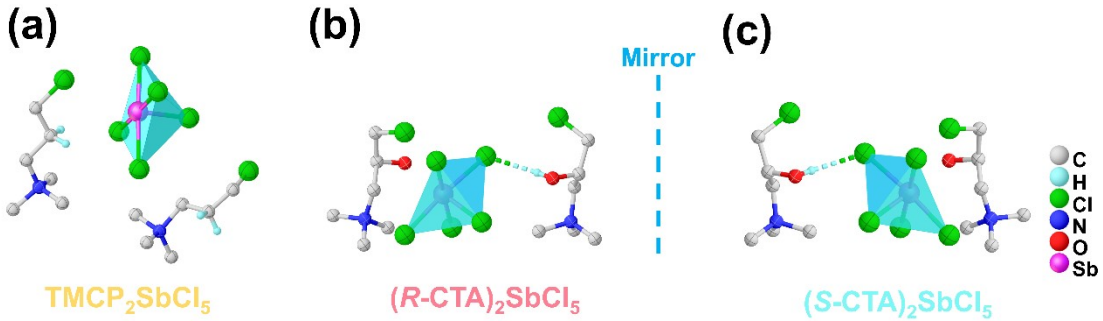

Fig. S4 Minimum asymmetric units of TMCP$_2$SbCl$_5$ (a), (R-CTA)$_2$SbCl$_5$ (b), and (S-CTA)$_2$SbCl$_5$ (c).

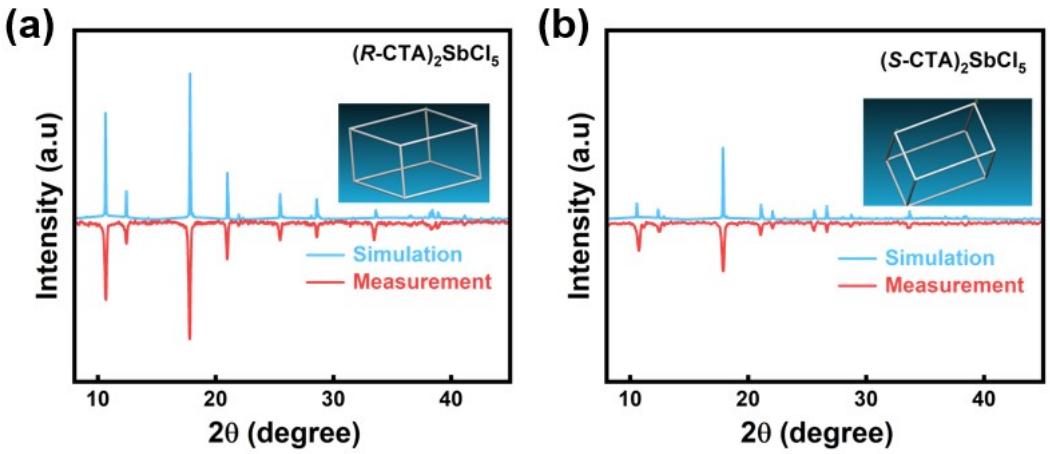

Fig. S5 Pawley refinement of PXRD data of (R-CTA)$_2$SbCl$_5$ (a) and (S-CTA)$_2$SbCl$_5$ (b) collected at 435 K with tetragonal crystal system.

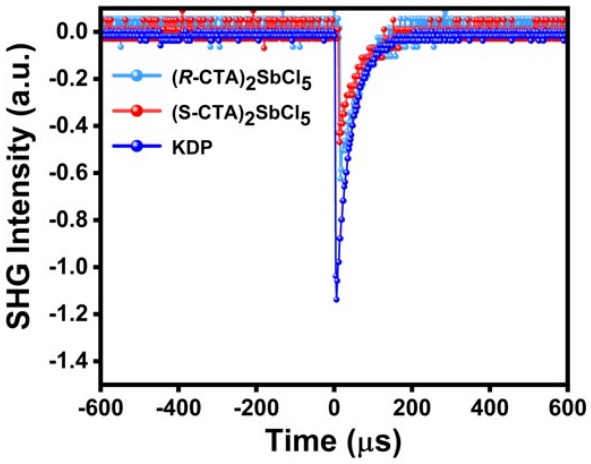

Fig. S6 The comparison of the SHG signals of (*R*/*S*-CTA)$_2$SbCl$_5$ with that of standard KDP at room temperature.

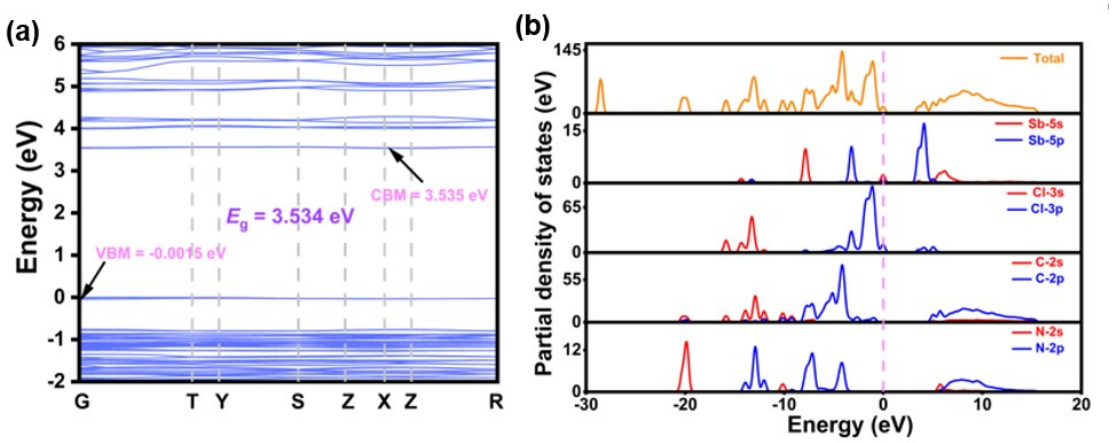

Fig. S7 The energy-band structure (a) and the partial density of states (PDOS) (b) of (*S*-CTA)$_2$SbCl$_5$

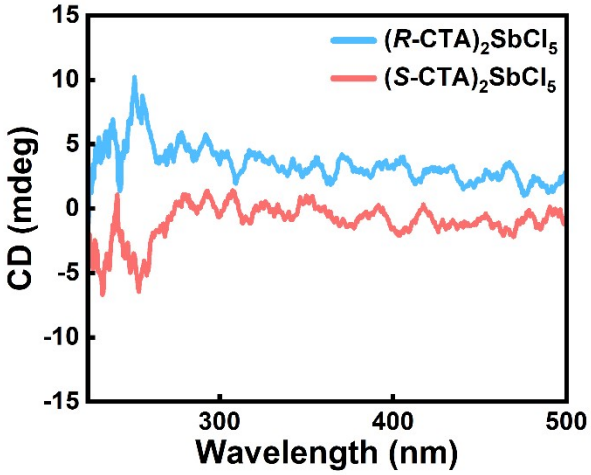

Fig. S8 CD spectra of (*R*/*S*-CTA)$_2$SbCl$_5$

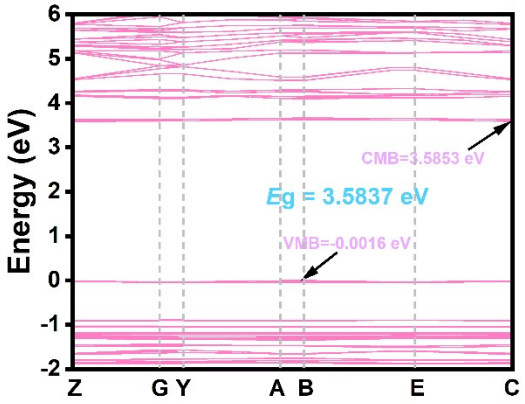

Fig. S9 The energy-band structure of $TMCP_2SbCl_5$

Table S1. Crystal data and structure refinement for (*R/S*-CTA)$_2$$SbCl_5$ at 293 K

	R-CTA_2SbCl_5	*S*-CTA_2SbCl_5
Empirical formula	$Cl_5Sb{\cdot}2(C_6H_{15}ClNO)$	$Cl_5Sb{\cdot}2(C_6H_{15}ClNO)$
Formula weight	604.28	604.28
Crystal system	Orthorhombic	Orthorhombic
Space group	$P2_12_12_1$	$P2_12_12_1$
a/Å	8.9032(3) Å	8.9021(2) Å
b/Å	9.5971(3) Å	9.5969(2) Å
c/Å	28.2922(8) Å	28.2865(7) Å
α/°	90	90
β/°	90	90
γ/°	90	90
Crystal size/mm^3	0.02 × 0.01 × 0.01	0.02 × 0.01 × 0.01
Volume/Å^3	2417.42(12) Å^3	2416.59(10) Å^3
Z	4	4
F(000)	1208	1208
Goodness-of-fit on F^2	1.03	1.03
R_1 [I>=2σ (I)]	0.032	0.021
R_2 [I>=2σ (I)]	0.065	0.048

Table S2. Crystal data and structure refinement for $TMCP_2SbCl_5$ at 293 K and 400 K

Temperature	239 K	400 K
Empirical formula	$Cl_5Sb{\cdot}2(C_6H_{15}ClN)$	$Cl_5Sb{\cdot}2(C_6ClN)$
Formula weight	572.28	542.05
Crystal system	Monoclinic	Monoclinic
Space group	$P2_1/c$	$P2_1/c$
a/Å	8.5967(4) Å	8.652(4) Å
b/Å	31.8060(15) Å	32.014(13) Å
c/Å	9.6375(5) Å	9.671(4) Å
α/°	90	90

β/°	115.487(6)	116.319(9)
γ/°	90	90
Crystal size/mm^3	0.15 × 0.1 × 0.1	0.11 × 0.12 × 0.13
Volume/Å^3	2378.7(2) Å^3	2401.1(18) Å^3
Z	4	4
F(000)	1144	1024.0
Goodness-of-fit on F^2	1.04	1.042
R_1 [I>=2σ (I)]	0.046	0.048
R_2 [I>=2σ (I)]	0.138	0.1524

Table S3. Bond Lengths and Bond Angles for (*R*-CTA)$_2$SbCl$_5$ at 293 K

Bond lengths [Å]			
Sb1—Cl1	2.6180 (11)	Cl7—C12	1.790 (5)
Sb1—Cl2	2.5604 (12)	O2—C11	1.418 (5)
Sb1—Cl3	2.5937 (10)	N2—C7	1.511 (5)
Sb1—Cl4	2.6993 (12)	N2—C8	1.488 (6)
Sb1—Cl5	2.3606 (10)	N2—C9	1.501 (6)
Cl6—C6	1.783 (5)	N2—C10	1.514 (5)
O1—C5	1.425 (5)	C4—C5	1.513 (5)
N1—C1	1.492 (6)	C5—C6	1.513 (6)
N1—C2	1.467 (6)	N1—C4	1.504 (5)
N1—C3	1.485 (5)		
Angles [°]			
Cl1—Sb1—Cl4	90.16 (4)	C5—C6—Cl6	112.6 (3)
Cl2—Sb1—Cl1	89.00 (4)	C7—N2—C10	107.1 (3)
Cl2—Sb1—Cl3	91.38 (4)	C8—N2—C7	107.2 (4)
Cl2—Sb1—Cl4	176.62 (4)	C8—N2—C9	110.4 (4)
Cl3—Sb1—Cl1	173.97 (4)	C8—N2—C10	112.4 (3)
Cl3—Sb1—Cl4	89.11 (4)	C9—N2—C7	108.2 (4)
Cl5—Sb1—Cl1	86.53 (4)	C9—N2—C10	111.3 (4)
Cl5—Sb1—Cl2	88.98 (4)	C1—N1—C4	110.7 (4)
Cl5—Sb1—Cl3	87.46 (4)	C2—N1—C1	109.7 (5)
Cl5—Sb1—Cl4	87.70 (4)	C2—N1—C3	108.2 (4)
C3—N1—C4	107.9 (3)	C2—N1—C4	112.9 (4)
N1—C4—C5	118.0 (3)	C3—N1—C1	107.3 (4)
O1—C5—C4	112.8 (3)	C11—C10—N2	115.7 (3)
O1—C5—C6	112.1 (4)	O2—C11—C10	108.7 (4)
C6—C5—C4	110.4 (3)	O2—C11—C12	111.0 (4)
N1—C4—C5	118.0 (3)	C12—C11—C10	110.6 (4)
O1—C5—C4	112.8 (3)	C11—C12—Cl7	113.1 (3)
O1—C5—C6	112.1 (4)	C11—C10—N2	115.7 (3)
C6—C5—C4	110.4 (3)	O2—C11—10	108.7 (4)
C12—C11—C10	110.6 (4)	O2—C11—C12	111.0 (4)
C11—C12—Cl7	113.1 (3)		

Table S4. Bond Lengths and Bond Angles for (*S*-CTA)$_2$SbCl$_5$ at 293 K

Bond lengths [Å]			
Sb1—Cl1	2.6178 (8)	Cl7—C12	1.786 (4)
Sb1—Cl2	2.5602 (9)	O2—C11	1.414 (4)
Sb1—Cl3	2.5926 (7)	N2—C7	1.490 (5)
Sb1—Cl4	2.6967 (9)	N2—C8	1.494 (5)
Sb1—Cl5	2.3616 (8)	N2—C9	1.469 (5)
Cl6—C6	1.789 (4)	N2—C10	1.510 (4)
O1—C5	1.407 (4)	C10—C11	1.512 (4)
N1—C1	1.506 (5)	C11—C12	1.520 (5)
N1—C2	1.494 (5)	C4—C5	1.518 (4)
N1—C3	1.493 (5)	C5—C6	1.511 (5)
N1—C4	1.511 (4)		
Angles [°]			
Cl1—Sb1—Cl4	90.14 (3)	C5—C6—Cl6	113.2 (3)
Cl2—Sb1—Cl1	88.99 (3)	C7—N2—C8	107.0 (3)
Cl2—Sb1—Cl3	91.42 (3)	C7—N2—C10	111.0 (3)
Cl2—Sb1—Cl4	176.59 (3)	C8—N2—C10	107.7 (2)
Cl3—Sb1—Cl1	173.99 (3)	C9—N2—C7	110.1 (4)
Cl3—Sb1—Cl4	89.11 (3)	C9—N2—C8	108.2 (4)
Cl5—Sb1—Cl1	86.56 (3)	C9—N2—C10	112.5 (3)
Cl5—Sb1—Cl2	88.94 (3)	O2—C11—C10	113.4 (3)
Cl5—Sb1—Cl3	87.45 (3)	C10—C11—C12	109.5 (3)
Cl5—Sb1—Cl4	87.72 (3)	C11—C12—Cl7	112.2 (2)
C1—N1—C4	106.9 (3)	C3—N1—C1	107.7 (3)
C2—N1—C1	108.7 (3)	C3—N1—C2	110.2 (3)
C2—N1—C4	111.1 (3)	C3—N1—C4	112.1 (3)
O1—C5—C4	109.2 (3)	N1—C4—C5	115.9 (3)
O1—C5—C6	111.4 (3)		

Table S5. Bond Lengths and Bond Angles for TMCP$_2$SbCl$_5$ at 293 K

Bond lengths [Å]			
Sb1—Cl3	2.6774 (12)	Cl2—C12	1.690 (9)
Sb1—Cl4	2.6640 (14)	N2—C7	1.503 (11)
Sb1—Cl5	2.5520 (13)	N2—C8	1.452 (10)
Sb1—Cl6	2.5619 (15)	N2—C9	1.445 (12)
Sb1—Cl7	2.3680 (14)	N2—C10	1.554 (12)
Cl1—C6	1.768 (5)	C10—C11	1.442 (8)
N1—C1	1.481 (9)	C11—C12	1.447 (12)
N1—C2	1.504 (6)	C5—C6	1.492 (7)
N1—C3	1.478 (8)	C4—C5	1.510 (7)
N1—C4	1.495 (6)		
Angles [°]			

Cl4—Sb1—Cl3	90.85 (5)	C5—C6—Cl1	109.9 (4)
Cl5—Sb1—Cl3	177.62 (5)	C7—N2—C10	98.4 (7)
Cl5—Sb1—Cl4	90.74 (5)	C8—N2—C7	111.6 (7)
Cl5—Sb1—Cl6	88.10 (5)	C8—N2—C10	113.3 (7)
Cl6—Sb1—Cl3	90.22 (5)	C9—N2—C7	109.5 (8)
Cl6—Sb1—Cl4	176.60 (6)	C9—N2—C8	110.0 (8)
Cl7—Sb1—Cl3	88.47 (5)	C9—N2—C10	113.5 (7)
Cl7—Sb1—Cl4	88.97 (7)	C11—C10—N2	115.0 (8)
Cl7—Sb1—Cl5	89.79 (6)	C10—C11—C12	117.6 (9)
Cl7—Sb1—Cl6	87.83 (7)	C11—C12—Cl2	124.4 (8)
C1—N1—C2	106.8 (5)	C4—N1—C2	107.8 (4)
C1—N1—C4	112.5 (5)	C6—C5—C4	110.8 (5)
C3—N1—C1	112.7 (7)	C3—N1—C4	109.6 (5)
C3—N1—C2	107.2 (5)		

Table S6. Bond Lengths and Bond Angles for $TMCP_2SbCl_5$ at 400 K

Bond lengths [Å]			
C1—N2	1.519 (15)	C11—N1	1.53 (2)
C1A—N2	1.520 (18)	C12—N1	1.44 (2)
C2—N2	1.534 (13)	C5A—C8A	1.47 (2)
C2A—N2	1.539 (16)	C5A—Cl5A	1.800 (17)
C3—N2	1.519 (15)	C6A—C8A	1.483 (14)
C3A—N2	1.522 (17)	C6A—N1A	1.510 (19)
C4—C9	1.468 (13)	C10A—N1A	1.49 (2)
C4—N2	1.505 (11)	C11A—N1A	1.53 (2)
C7—C9	1.521 (14)	C12A—N1A	1.44 (2)
C7—Cl2	1.754 (10)	Cl1—Sb1	2.654 (2)
C5—C8	1.468 (19)	Cl3—Sb1	2.548 (2)
C5—Cl5	1.797 (15)	Cl4—Sb1	2.665 (2)
C6—C8	1.498 (9)	Cl6—Sb1	2.352 (2)
C6—N1	1.513 (17)	Cl7—Sb1	2.541 (2)
C10—N1	1.486 (19)		
Angles [°]			
C9—C4—N2	111.3 (9)	C12—N1—C10	108.0 (16)
C9—C7—Cl2	105.6 (7)	C12—N1—C11	116.0 (16)
C4—C9—C7	108.7 (9)	C8A—C5A—Cl5A	125 (3)
C1—N2—C2	104.6 (14)	C8A—C6A—N1A	115 (2)
C1A—N2—C2A	112.3 (14)	C5A—C8A—C6A	120 (3)
C1A—N2—C3A	113.1 (13)	C6A—N1A—C11A	117 (2)
C3—N2—C1	112.4 (16)	C10A—N1A—C6A	116 (2)
C3—N2—C2	103.8 (14)	C10A—N1A—C11A	106 (2)
C3A—N2—C2A	112.1 (14)	C12A—N1A—C6A	99 (2)
C4—N2—C1	121.2 (17)	C12A—N1A—C10A	104 (3)
C4—N2—C1A	102 (2)	C12A—N1A—C11A	114 (3)
C4—N2—C2	107.4 (13)	Cl1—Sb1—Cl4	91.08 (8)

C4—N2—C2A	99 (2)	Cl3—Sb1—Cl1	177.16 (9)
C4—N2—C3	106.0 (15)	Cl3—Sb1—Cl4	89.97 (8)
C4—N2—C3A	118 (3)	Cl6—Sb1—Cl1	89.01 (10)
C8—C5—Cl5	120.1 (12)	Cl6—Sb1—Cl3	88.37 (11)
C8—C6—N1	111.7 (15)	Cl6—Sb1—Cl4	88.63 (8)
C5—C8—C6	118.8 (14)	Cl6—Sb1—Cl7	89.85 (9)
C6—N1—C11	114.5 (13)	Cl7—Sb1—Cl1	90.62 (8)
C10—N1—C6	113.2 (13)	Cl7—Sb1—Cl3	88.27 (9)
C10—N1—C11	104.7 (14)	Cl7—Sb1—Cl4	177.70 (8)
C12—N1—C6	100.7 (14)		